Polym. Bull. (2012) 68:983–992
DOI 10.1007/s00289-011-0593-x

ORIGINAL PAPER

Preparation and properties of raw lacquer/multihydroxyl polyacrylate/organophilic montmorillonite nanocomposites

Yanlian Xu · Qinhui Chen · Weibin Bai · Jinhuo Lin

Received: 21 June 2011 / Revised: 28 July 2011 / Accepted: 30 July 2011 /
Published online: 18 August 2011

Abstract Raw lacquer (RLA) has been widely used indoors for centuries in Asia. But its weak UV-resistant property limited its outdoor application. In this article, the UV-resistant property of lacquer film was significantly improved by solution intercalation method. The intercalated nanocomposites were obtained from RLA, multihydroxyl polyacrylate resin (MPA), and organophilic montmorillonite (OMMT). The structure and morphology of the RLA/MPA/OMMT nanocomposites were confirmed by X-ray diffraction (XRD), transmission electron microscopy (TEM), and scanning electron microscopy (SEM). The variation of the film gloss and impact strength with different UV exposure time was also investigated. Owing to the dispersion of nanometer-sized OMMT in polymer matrix, the RLA/MPA/OMMT nanocomposites exhibited improved UV-resistant property. When the OMMT content is 3.0 wt%, the best physical–mechanical properties can be obtained. These results indicated that the solution intercalation with nanoparticles was an efficient and convenient method to improve the properties of raw lacquer.

Keywords Raw lacquer · Montmorillonite · Nanocomposites · UV-resistant property

Introduction

Polymer nanocomposites have attracted great attention because of the dramatically enhanced material properties of polymers by incorporating layered silicates at fairly low concentrations [1]. Smectite clays, such as montmorillonite (MMT), were

Y. Xu · Q. Chen · W. Bai · J. Lin
College of Chemistry and Materials, Fujian Normal University, Fuzhou 350007, China

Y. Xu · Q. Chen · W. Bai · J. Lin (✉)
Fujian Key Laboratory of Polymer Materials, Fujian Normal University, Fuzhou 350007, China
e-mail: jhlin@fjnu.edu.cn

valuable minerals and widely used in many industrial applications because of their high aspect ratio, plate morphology, natural abundance, and low cost [2–10]. They were expandable layered silicates and could be intercalated or exfoliated into polymer. Following the success of nylon–organophilic montmorillonite (OMMT) nanocomposites [11] and nylon 6–clay hybrid [12, 13], polymer/MMT nanocomposites have received considerable attention in fundamental research, as well as in industrial exploitation in the past few years because of their improved mechanical properties, thermal- and photo-stability [14, 15], compared with the original polymers. Application performances, especially UV-resistant property and durability, which decide their useful lifetime of products in outdoor applications, are the key feature of any composite material.

Raw lacquer (RLA), a natural renewable and an eco-friendly biopolymer material, has been widely used in Asia to coat the objects of art and craft work for more than 5000–7000 years [16–18], because of its excellent physico-chemical properties, such as thermo-stability, anticorrosion, super-high durability, toughness, and brilliance [19, 20]. Many efforts have been achieved in this field to modify RLA [21–25]. RLA and most of its modified products, however, are mainly used indoors, for the lacquer films are more sensitive against UV radiation [26].

Previously, we have reported the preparation and properties of urushiol–titanium polymer (PUTi)/OMMT nanocomposite, and found that the PUTi/OMMT nanocomposites have good thermal stability and ultraviolet resistance [27]. In this study, RLA/Multihydroxyl polyacrylate resin (MPA)/OMMT nanocomposites were prepared in order to improve the UV-resistant property of raw lacquer. The nanocomposites may have potential applications in many fields such as outdoor sculpture and cultural relic restoration, etc. The structure and morphology of RLA/MPA/OMMT nanocomposites were elucidated by X-ray diffraction (XRD) and transmission electron microscopy (TEM). The influences of OMMT on the UV-resistant property of RLA/MPA/OMMT nanocomposites were investigated.

Experimental

Materials

Raw lacquer was obtained from the Xi'an Institute of Lacquer and Coating, China. Multihydroxyl polyacrylate resin (MPA) BS965 was purchased from Jiangsu Sanmu Group Corporation. Solid content%: 65 ± 2, Viscosity s, 25 °C (Gradner): 30–65, OH value (per solid): 85.8 ± 3.3, Acid value mgKOH/g: ≤10. OMMT (Model: BP–183) was obtained from Zhejiang Huate Group (China). Water degree (2 h, 105 °C): ≤3.50%, Granularity (over 0.076 mm): ≥95%, accumulated density: 350–450 G/L, Losing (1000 °C): ≤34%.

Preparation of RLA/MPA/OMMT nanocomposites

RLA/MPA/OMMT nanocomposites containing different amount of OMMT powders were prepared in our laboratory. In a typical experiment, 0.202 g of OMMT

Table 1 Some physical–mechanical properties of RLA/MPA/OMMT films

Sample	1	2	3	4	5
W_{OMMT} (%)	0	1.0	3.0	5.0	10.0
Touch-free dry/min	65	60	60	54	50
Hardened dry/h	18	18	17	17	15.5
Adhesion/grade	2	1	1	1	2
Hardness	2H	2H	3H	3H	2H
Brightness/%	102	100	100	95	85
Impact strength/kg·cm	40	45	50	50	40

powders was immerged in pure xylene for 24 h and the suspension was sonicated for 30 min, and then 4.0 g of MPA was added under stirring. The mixture was stirred with a magnetic stirrer for 10 min, and then 16.0 g of RLA was added to the solution. After being stirred for 24 h at room temperature in a closed container, the sample 2 was obtained. By changing the OMMT amount, we obtained samples 1, 3, 4, and 5 (see Table 1). The obtained solution was dropped on glass, then flowed and leveled to form sample films with thickness of ca. 30–40 μm. The nanocomposite films were dried under ambient atmosphere for 48 h. Some physical–mechanical properties of RLA/MPA/OMMT films were summarized in Table 1. The results showed that the properties of RLA/MPA/OMMT films were influenced by the OMMT content. The touch-free dry and hardened dry time both shortened due to the introduction of OMMT. The adhesion and hardness increased first, and then decreased with the increase of the content of OMMT. After overall consideration for all properties, the structure, morphology, and UV-resistant property of sample 3 were studied in detail.

Characterization of RLA/MPA/OMMT nanocomposites

XRD patterns were obtained by a Philips Analytical X'Pert–MPD (40 kV/30 mA) diffractometer with Cu–Kα radiation (λ = 0.154 nm) at room temperature. The scanning range was 1.0–8.0° at a rate of 2°/min. The fracture morphologies of the films were observed by scanning electron microscopy [SEM, Amray 1000B (Amray Co. USA)]. The TEM images were recorded on a JEM–2000EX instrument.

Some physical–mechanical properties tests were as follows:

According to GB/T 1728-1989 (China), the drying process of RLA/MPA/OMMT films can be divided into touch-free dry and hardened dry, which is measured using an automatic drying time recorder (QGZ-24 auto-recorder of painting drying time, Jinke, Tianjin, China).The adhesion was determined by pushing the coated panel beneath a rounded stylus of the QFZ Coating Adhesion Test Instrument until the coating was removed from the substrate surface under the GB/T 1720-1979 (1989, China) standard. The impact strength was determined by dropping a dart onto the center of the test specimen from varied drop heights of the film 0153-3 KI impact tester. The drop heights and the test fail results were recorded as the GB/T 1732-1993 (China). The brightness of the films was tested from the intensity of the

specular reflectance, compared with that of a standard surface of a black glass by QZX-60A Glossmeter under the GB/T 1743-1979 (China) standard. The hardness of the samples was measured with pencil hardness testing. According to GB/T 6739-1996 (China), the meanings of H designate how hard the tested films are. A higher number with H expresses the hardness of the tested films.

UV exposure test

The samples were exposed to a mercury lamp of 253 nm wavelength and 30 W power capacity under ambient atmosphere, and the surface of the films was 10 cm from the lamp envelope. The brightness loss rate and the impact strength holding rate of the films after the UV degradation were calculated using the following equations:

$$\text{Brightness loss rate}\,(\%) = (\mathrm{B}_0 - \mathrm{B}_t)/\mathrm{B}_0 \times 100\%.$$

$$\text{Impact strength holding rate}\,(\%) = (\mathrm{I}_t/\mathrm{I}_0) \times 100\%.$$

where B_0 was the brightness of films before UV exposure, and B_t was the brightness of films after UV exposure; I_0 was the impact strength of films before UV exposure, and I_t was the impact strength of films after UV exposure.

Results and discussion

The XRD patterns of RLA/MPA/OMMT nanocomposites

There are two complimentary techniques to characterize the structure of nanocomposites: XRD and TEM [28], where the former reveals the change of *d*-spacing of clay gallery while the later shows the morphological structure of nanocomposites.

Figure 1 shows the XRD patterns of OMMT and RLA/MPA/OMMT nanocomposites. In the XRD pattern of OMMT (see Fig. 1 curve "c"), there was a strong diffraction peak at 2θ =4.14°, which represented the diffraction from the (001) crystal surface of OMMT, corresponding to the *d*-spacing of 2.13 nm based on Bragg's equation. In Fig. 1 curve "a" and "b" (OMMT content 3.0 and 5.0 wt%, respectively), there were no obvious diffraction peaks within 2θ = 1–8°, which indicated that OMMT in the RLA/MPA matrix was exfoliated or intercalated. There was a dislocated peak at 2θ = 3.0°, which represented the diffraction from the (001) crystal surface of intercalated OMMT, corresponding to the average *d*-spacing of 2.94 nm.

TEM photographs of RLA/MPA/OMMT nanocomposites

Figure 2 shows the TEM photographs of RLA/MPA/OMMT nanocomposite containing 3.0 wt% OMMT. The dark region and the white region represented the OMMT phase and the RLA/MPA phase, respectively. The intercalated (Fig. 2a) and exfoliated (Fig. 2b) structure of OMMT could be clearly observed in the

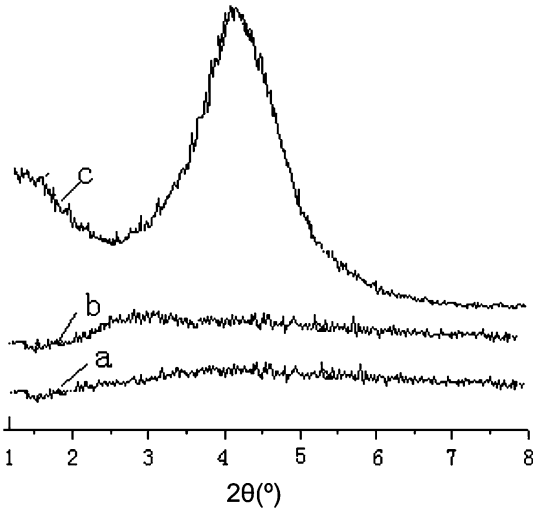

Fig. 1 XRD patterns of RLA/MPA/OMMT nanocomposites: *a* OMMT % = 3.0 wt%, *b* OMMT % = 5.0 wt%, *c* OMMT % = 100 wt%

RLA/MPA/OMMT matrix, and the *d*-spacing between the layers of intercalated OMMT was more than 10 nm. And these were in good agreement with the results of XRD.

SEM photographs of RLA/MPA/OMMT nanocomposites

Raw lacquer, a water-in-oil emulsion, consists of the "oily," or urushiol, fraction (about 65%) and an aqueous fraction (35%). The caves were the marks of waterdrops in the raw lacquer [24, 29]. The SEM images of the cross-section of RLA, RLA/MPA, and RLA/MPA/OMMT (3.0 wt%) films were shown in Fig. 3. In Fig. 3a, b the emulsion micelle ("cave") was observed although a relative flat surface was observed in Fig. 3c. The similar caves between RLA and RLA/MPA were considered that a small quantity of MPA was dispersed among the "oily" urushiol matrix and MPA did not changed the emulsion structure of RLA. However, the OMMT changed the emulsion structure of RLA, because it has both hydrophilic and hydrophobic groups, which resulted in the different morphology between RLA/MPA and RLA/MPA/OMMT. The SEM results showed that a small quantity of MPA did not change the emulsion structure of RLA, but the OMMT was on the contrary.

UV exposure test

The RLA, RLA/MPA, and RLA/MPA/OMMT films were set at 10 cm from a UV lamp (253 nm, 30 W) under ambient atmosphere, all samples tested after laying aside for 48 h.

Figures 4 and 5 show the UV exposure effect on the brightness and impact strength of the films, respectively. Brightness and impact strength were important

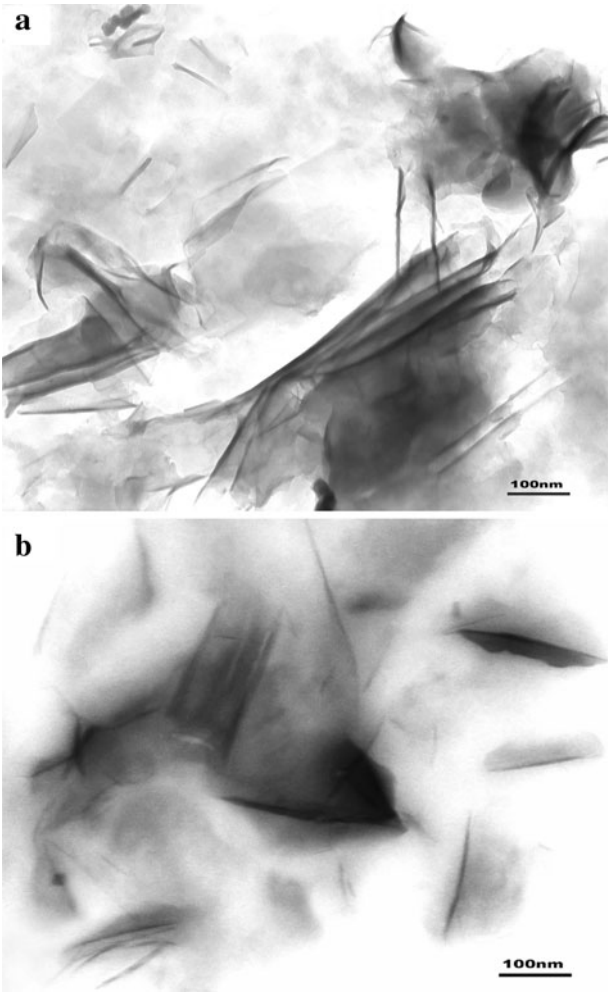

Fig. 2 TEM images of RLA/MPA/OMMT (3.0 wt%)

factor in the aging of RAL films. The brightness loss rate of the surface increased considerably with exposure time. Addition of 3.0% OMMT to RLA/MPA reduced brightness loss rate from 22.5 to 15.0% at 384 h. Addition of 3.0% OMMT to RLA/MPA remarkably increased the impact strength holding rate from 20 to 50%. For RLA and RLA/MPA films, there were no obvious differences in brightness loss and impact strength holding rate with increasing of exposure time. These results demonstrated that the UV-resistant property of the RLA films was improved due to the introduction of OMMT.

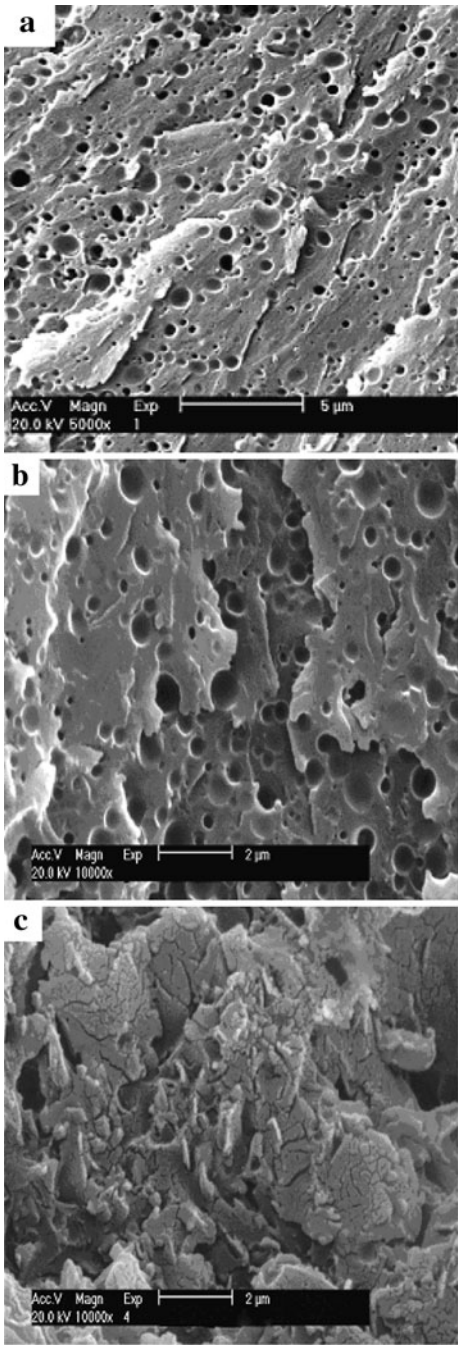

Fig. 3 Cross-section SEM images of **a** RLA, **b** RLA/MPA, and **c** RLA/MPA/OMMT (3.0 wt%) dried at room temperature, about 70% relative humidity (RH) for 7 days

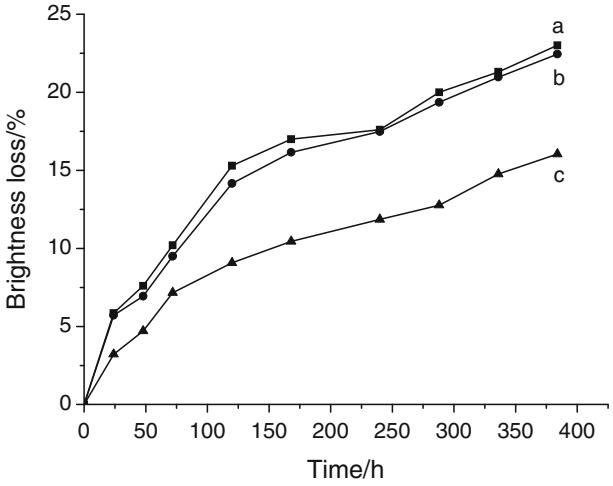

Fig. 4 UV exposure effect on brightness of *a* RLA, *b* RLA/MPA, *c* RLA/MPA/OMMT (3.0 wt%)

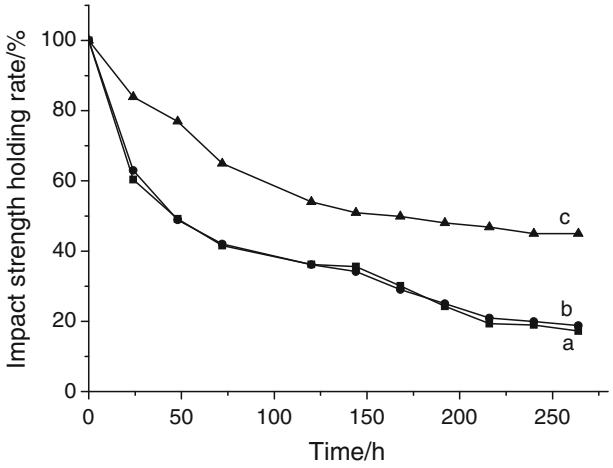

Fig. 5 UV exposure effect on impact strength of *a* RLA, *b* RLA/MPA, *c* RLA/MPA/OMMT (3.0 wt%)

Conclusion

By employing the solution intercalation method, RLA/MPA/OMMT nanocomposites were successfully prepared, as confirmed by XRD and TEM. The aging resistance for the intercalation nanocomposites was increased compared with that of the original RLA film, indicating that the nanocomposites could be potentially used outdoors. Totally, this article demonstrates the solution intercalation with nanoparticles was an efficient and convenient approach to improve the UV-resistant properties of materials.

Acknowledgments This study was supported by the National Natural Science Foundation of China (51073037, 50973020), and the Natural Science Foundation of Fujian, China (2010J01030).

References

1. Pavlidoua S, Papaspyrides CD (2008) A review on polymer–layered silicate nanocomposites. Prog Polym Sci 33:1119–1198
2. Li X, Zhan ZJ, Peng GR, Wang WK (2011) A new method for preparing completely exfoliated epoxy/clay nanocomposites: nano-disassembling method. Polym Bull. doi:10.1007/s00289-011-0496-x
3. Mohsen-Nia M, Mohammad Doulabi FS (2011) Synthesis and characterization of polyvinyl acetate/montmorillonite nanocomposite by in situ emulsion polymerization technique. Polym Bull 66:1255–1265
4. Garces JM, Moll DJ, Bicerano J, Fibiger R, McLeod DG (2000) Polymeric nanocomposites for automotive applications. Adv Mater 12:1835–1839
5. Bao Y, Ma JZ (2011) Polymethacrylic acid/Na-montmorillonite/SiO_2 nanoparticle composites structures and thermal properties. Polym Bull 66:541–549
6. Meng XY, Wang Z, Zhao ZF, Du XH, Bi WG, Tang T (2007) Morphology evolutions of organically modified montmorillonite/polyamide 12 nanocomposites. Polymer 48:2508–2519
7. Da Silva PA, Jacobi MM, Schneider LK, Oliveira RVB, Mauler RS, Barbosa RV, Coutinho PA (2010) SBS nanocomposites as toughening agent for polypropylene. Polym Bull 64:245–257
8. Tsai TY, Li CH, Chang CH, Cheng WH, Hwang CL, Wu RJ (2005) Preparation of exfoliated polyester/clay nanocomposites. Adv Mater 17:1769–1773
9. Choi YS, Wang KH, Xu MZ, Chung IJ (2002) Synthesis of exfoliated polyacrylonitrile/Na−MMT nanocomposites via emulsion polymerization. Chem Mater 14:2936–2939
10. Nam BU, Son Y (2010) Evaluations of PP-g-GMA and PP-g-HEMA as a compatibilizer for polypropylene/clay nanocomposites. Polym Bull 65:837–847
11. Usuki A, Mizutani T, Fukushima Y, Fujimoto M, Fukumori K, Kojima Y, Sato N, Kurauchi T, Kamigaito O, 1989, U.S. Pat., 4.889.885
12. Okada A, Kawasumi M, Kurauchi T, Kamigaito O (1987) Synthesis and characterization of a nylon-6-clay hybrid. Polym Prepr 28:447–448
13. Kojima Y, Usuki A, Kawasumi M, Okada A, Fukushima Y, Kurauchi T, Kamigaito O (1993) Mechanical properties of nylon 6-clay hybrid. J Mater Res 8:1185–1189
14. Tian HY, Tagaya H (2008) Dynamic mechanical property and photochemical stability of perlite/PVA and OMMT/PVA nanocomposites. J Mater Sci 43:766–770
15. Zhu SP, Chen JY, Li HL (2009) Influence of poly(ethylene glycol)/montmorillonite hybrids on the rheological behaviors and mechanical properties of polypropylene. Polym Bull 63:245–257
16. Kumanotani J (1995) Urushi (oriental lacquer)—a natural aesthetic durable and future–promising coating. Prog Org Coat 26:163–195
17. Niimura N, Miyakoshi T (2006) Structural study of oriental lacquer films during the hardening process. Talanta 70:146–152
18. Langhals H, Bathelt D (2003) The restoration of the largest archaelogical discovery—a chemical problem: conservation of the polychromy of the Chinese Terracotta Army in Lintong. Angew Chem Int Ed 42:5676–5681
19. Kim HS, Yeum JH, Choi SW, Lee JY, Cheong IW (2009) Urushiol/polyurethane–urea dispersions and their film properties. Prog Org Coat 65:341–347
20. Xia JR, Lin JH, Xu YL, Chen QH (2011) On the UV-induced polymeric behavior of Chinese lacquer. ACS Appl Mater Interfaces 3:482–489
21. Hu BH, Chen WD, Lin JH (1998) Pilot research on new type anticorrosive coating of urushiol-titanium chelate polymer. Chem Ind Forest Prod 18:17–22
22. Hu BH, Chen WD, Lin JH (1993) The synthesis of urushiol titanium chelate polymers and their structural characteristics. Chin J Polym Sci 11:198–203
23. Nagase K, Lu R, Miyakoshi T (2004) Studies on the fast drying hybrid Urushi in low humidity environment. Chem Lett 33:90–91
24. Lu R, Harigaya S, Ishimura T, Nagase K, Miyakoshi T (2004) Development of a fast drying lacquer based on raw lacquer sap. Prog Org Coat 51:238–243

25. Ishimura T, Lu R, Miyakoshi T (2006) Studies on the reaction mechanism between urushiol and organic silane. Prog Org Coat 55:66–69
26. Ogawa T, Arai K, Osawa S (1998) Light stability of oriental lacquer films irradiated by a fluorescent lamp. J Environ Polym Degrad 6:59–65
27. Xu YL, Hu BH, Lin JH, Xiao P (2005) Preparation and properties of urushiol-titanium polymer/organomontmorillonite nanocomposites. Acta Polym Sin 825–828
28. Ray SS, Okamoto M (2003) Polymer/layered silicate nanocomposites: a review from preparation to processing. Prog Polym Sci 28:1539–1641
29. Kumanotani J (1997) Enzyme catalyzed durable and authentic oriental lacquer: a natural microgel-printable coating by polysaccharide–glycoprotein–phenolic lipid complexes. Prog Org Coat 34:135–146